Proceedings of the 17th World Congress
The International Federation of Automatic Control
Seoul, Korea, July 6-11, 2008

Potential of Low Bandwidth Active Suspension Control with Continuously Variable Damper

Guido Koch * **Oliver Fritsch** * **Boris Lohmann** *

* *Institute of Automatic Control, Technische Universität München, D-85748 Garching, Germany (Tel: +49-89-28915663; e-mail: guido.koch@tum.de, oliver.fritsch@mytum.de, lohmann@tum.de).*

Abstract: Due to rising customer demands for driving comfort, the integration of controlled active and semi-active elements in modern vehicle suspension systems has increased considerably. A significant number of upper class vehicle suspensions is either equipped with continuously variable dampers or low bandwidth actuators. However, the combination of these suspension elements is not applied so far. In this paper active quarter car models are used to design time-invariant LQR controllers for specific road conditions. By optimizing the controller weights and damping ratio based on a new iterative optimization procedure, the potential of road adaptive low bandwidth systems with continuously variable dampers is clearly highlighted. It is shown that ride comfort can be significantly increased while satisfying given constraints for ride safety (maximum tire deflections) and suspension travel. The achievable performance is compared to passive and high bandwidth active suspension systems using carpet plots.

Keywords: Active and semi-active vehicle suspensions; Vehicle dynamics; Vehicles control; Multi-objective optimization; Active vibration control.

1. INTRODUCTION

The requirements regarding suspension systems of modern automobiles are constantly increasing. On the one hand, the vehicle should provide an optimum of drive comfort, on the other hand, the vehicle should be safely driveable all the time. This safety aspect requires a stiff, well damped coupling between the vehicle and the road, especially for non-stationary driving maneuvers, e.g. driving a rough road or cornering. A simple measure for ride comfort is the normalized [1] root mean square (rms) chassis acceleration and the normalized rms tire deflection is a measure for ride safety. In every driving state, both values should be as low as possible for optimal performance of the suspension. However, Figure 1 shows the conflict of objectives occurring for a typical passive suspension (parameters according to Table 1), Mitschke and Wallentowitz (2004). In this case the optimal body damping ratio ζ_b regarding handling is approximately 0.40. Optimal comfort in contrast can be achieved with a body damping ratio of about 0.16.

Application of active suspension systems can ease this conflict between comfort and safety by the integration of actuators. But the application of high bandwidth actuators in production vehicles still fails due to high energy demands and costs. Still, in modern upperclass vehicles active hardware is already included: On the one hand there are semiactive elements like dampers with continuously variable damping characteristic (e.g. magnetorheological dampers) which offer the advantage of low energy demands, Canale et al. (2006). On the other hand active

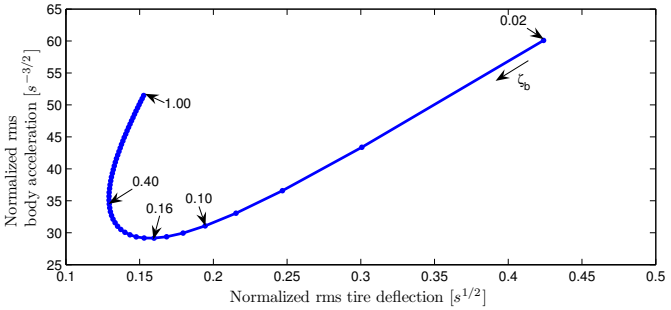

Fig. 1. Conflicting objectives for a passive suspension

systems like low bandwidth hydraulic systems actively damp vertical chassis vibrations up to approx. 5 Hz, Pyper et al. (2003). However so far, the systems are not combined in production.

The focus of this paper is the performance analysis of differently damped, time-invariant, low bandwidth active suspension (LBAS) systems. Therefore, a new iterative optimization procedure based on the insights of Sharp and Hassan (1987) and Hrovat (1997) is utilized. In Section 2 linear high and low bandwidth active suspension models are presented as well as a stochastic disturbance model for the road induced vibrations. The LQR controller design is presented in Section 3. In Section 4 follows the analysis of the influence of actuator bandwidth and damping for the LQR-controlled LBAS. The insights gained are used in Section 5 to analyze potential performance benefits of an adaptive controller for an LBAS with continuously variable damper.

[1] The normalization to the disturbance noise intensity is presented in detail in Section 4.1.

2. ACTIVE SUSPENSION MODELS

If only the vehicle's vertical dynamic primary degree of freedom, i.e. the vertical translatory movement, is considered, the vehicle suspension can be modelled by the well-known quarter-car model, as described by Wong (2001), Mitschke and Wallentowitz (2004).

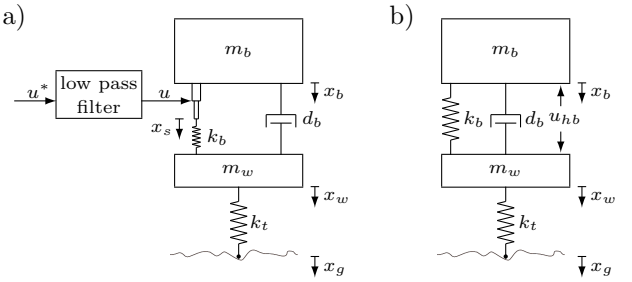

Fig. 2. a) LBAS model b) HBAS model

2.1 Low bandwidth active suspension

The quarter car model of the LBAS is shown in Figure 2a). The displacement generating actuator acting in series with the main suspension spring is considered to be ideal, i.e. the actuator instantly produces the displacements requested by the signal u. All bandwidth limitations of the actuator are represented by a second order low pass filter filtering the desired control input u^*. The low pass filter's cut-off frequency ω_c and the damping ratio of the body $\zeta_b = d_b/(2\sqrt{k_b m_b})$ are fixed for any particular set of performance calculations but these are carried out for a wide range of values for ω_c and ζ_b. The definitions and values of the parameters used are given in Table 1. With the ideal actuator assumption $u = x_b - x_s$ the equations of motion can be written as

$$m_b\ddot{x}_b = -k_b(x_b - x_w) + k_b u - d_b(\dot{x}_b - \dot{x}_w), \tag{1}$$
$$m_w\ddot{x}_w = k_b(x_b - x_w) - k_b u + d_b(\dot{x}_b - \dot{x}_w) - k_t(x_w - x_g).$$

Introducing the state vector $\mathbf{x}$ and output vector $\mathbf{y}$

$$\mathbf{x} = \begin{bmatrix} x_1 \\ x_2 \\ x_3 \\ x_4 \end{bmatrix} = \begin{bmatrix} x_b - x_w \\ x_w - x_g \\ \dot{x}_b \\ \dot{x}_w \end{bmatrix}, \quad \mathbf{y} = \begin{bmatrix} y_1 \\ y_2 \\ y_3 \end{bmatrix} = \begin{bmatrix} \ddot{x}_b \\ x_b - x_w \\ x_w - x_g \end{bmatrix} \tag{2}$$

the state space representation becomes

$$\begin{aligned} \dot{\mathbf{x}} &= \mathbf{A}\mathbf{x} + \mathbf{b}u + \mathbf{g}\dot{x}_g \,, \\ \mathbf{y} &= \mathbf{C}\mathbf{x} + \mathbf{d}u \,, \end{aligned} \tag{3}$$

where

$$\mathbf{A} = \begin{bmatrix} 0 & 0 & 1 & -1 \\ 0 & 0 & 0 & 1 \\ -\omega_b^2 & 0 & -2\zeta_b\omega_b & 2\zeta_b\omega_b \\ \frac{\omega_b^2}{\rho} & -\omega_w^2 & \frac{2\zeta_b\omega_b}{\rho} & -\frac{2\zeta_b\omega_b}{\rho} \end{bmatrix}, \quad \mathbf{b} = \begin{bmatrix} 0 \\ 0 \\ \omega_b^2 \\ -\frac{\omega_b^2}{\rho} \end{bmatrix},$$

$$\mathbf{g} = \begin{bmatrix} 0 \\ -1 \\ 0 \\ 0 \end{bmatrix}, \; \mathbf{C} = \begin{bmatrix} -\omega_b^2 & 0 & -2\zeta_b\omega_b & 2\zeta_b\omega_b \\ 1 & 0 & 0 & 0 \\ 0 & 1 & 0 & 0 \end{bmatrix}, \; \mathbf{d} = \begin{bmatrix} \omega_b^2 \\ 0 \\ 0 \end{bmatrix}.$$

These state space equations describe the system dynamics without the bandwidth limitation. The inputs of the system are the actual displacement of the actuator u and the state disturbance $\dot{x}_g$, which is the vertical ground velocity. The outputs of the system are the vertical body acceleration y_1, the suspension deflection y_2, and the tire deflection y_3. The low pass filter is described by

$$\ddot{u} + 2\zeta_f\omega_c\dot{u} + \omega_c^2 u = \omega_c^2 u^*, \tag{4}$$

where the cut-off frequency ω_c incorporates the bandwidth of the actuator. By augmenting (3) with the additional states u and $\dot{u}$ from (4) a sixth order state space representation can be derived, that describes the whole system shown in Figure 2a), including the filter. The new control input to the system becomes the desired actuator deflection u^*.

Table 1. Notation and parameter values

Model parameter	Symbol	Value	Unit
Quarter car body mass	m_b	320	[kg]
Wheel assembly mass	m_w	32	[kg]
Mass ratio	$\rho = \frac{m_w}{m_b}$	0.10	[–]
Suspension spring stiffness	k_b	13000	[N/m]
Tire stiffness	k_t	127000	[N/m]
Body damping ratio	$\zeta_b = \frac{d_b}{2\sqrt{k_b m_b}}$	varying	[–]
Low pass filter damping ratio	ζ_f	$\frac{1}{\sqrt{2}} \approx 0.707$	[–]
Undamped uncoupled natural frequency of the body	$\omega_b = \sqrt{\frac{k_b}{m_b}}$	6.37	[rad/s]
Uncoupled natural frequency of the tire	$\omega_t = \sqrt{\frac{k_t}{m_w}}$	63.0	[rad/s]
Low pass filter cut-off frequency	ω_c	varying	[rad/s]

2.2 High bandwidth active suspension

Figure 2b) shows a high bandwidth active suspension (HBAS) with a force generating actuator mounted in parallel to the spring and the damper. In the following description no bandlimit is considered for the HBAS such that it can be treated as a performance benchmark for the LBAS in the analysis in Sections 4 and 5.

With u_{hb} being the actuator force, the equations of motion can be derived as

$$m_b\ddot{x}_b = -k_b(x_b - x_w) - d_b(\dot{x}_b - \dot{x}_w) - u_{hb} \,, \tag{5}$$
$$m_w\ddot{x}_w = k_b(x_b - x_w) + d_b(\dot{x}_b - \dot{x}_w) - k_t(x_w - x_g) + u_{hb} \,.$$

By introducing the same states as in (2) one can transfer (5) into a state space representation, where the matrix $\mathbf{A}$ and the vector $\mathbf{g}$ are identical to those of (3). Between the vector $\mathbf{b}_{hb}$ of the HBAS model and the vector $\mathbf{b}$ of the LBAS model exists the relationship

$$\mathbf{b} = \begin{bmatrix} 0 \\ 0 \\ \omega_b^2 \\ -\frac{\omega_b^2}{\rho} \end{bmatrix} = \begin{bmatrix} 0 \\ 0 \\ \frac{k_b}{m_b} \\ -\frac{\frac{k_b}{m_b}}{\frac{m_w}{m_b}} \end{bmatrix} = -k_b \begin{bmatrix} 0 \\ 0 \\ -\frac{1}{m_b} \\ \frac{1}{m_w} \end{bmatrix} = -k_b\mathbf{b}_{hb} \,. \tag{6}$$

Thus, if all model parameters are chosen identically the HBAS and the LBAS *without* the low pass filter behave equivalently if

$$-k_b u = u_{hb}, \qquad \forall t \geq t_0 \tag{7}$$

holds. That means that despite of the different mechanical structure, both systems offer the same performance and taking the bandlimit into account the performance of the LBAS tends towards the performance of the HBAS, when the filter cut-off frequency is increasing.

2.3 Disturbance model

The suspension system is disturbed by random road induced vibrations. The state disturbance is therefore modeled appropriately by a stationary random process. As Hrovat (1997) states, a frequently used approximation of a road displacement power spectral density is given by

$$S_{x_g}(\omega) = \frac{1}{v} A \left(\frac{\omega}{v}\right)^n, \tag{8}$$

where A is a constant roughness factor in [m], ω is the angular frequency in [rad/s] and v is the constant vehicle velocity in [m/s]. For the parameter n we assume a value of -2. This implies the commonly used assumption of white noise for the vertical ground velocity and hence a constant power spectrum $S_{\dot{x}_g} = \omega^2 \cdot S_{x_g} = Av$ depending on road conditions and driving speed.

3. SUSPENSION CONTROLLER DESIGN

Since the focus of the paper is the determination of the potential of LBASs with variable damping rather than sophisticated controller design, a linear control structure is used that provides good insight in the closed loop system behavior. The white noise assumption for the disturbance signal $\dot{x}_g$ meets the requirements for the application of linear stochastic control theory as it is presented for instance in Kwakernaak and Sivan (1972).

The controller is designed for the fourth order system (3) using linear quadratic regulator (LQR) design techniques. Thus, it is assumed that all states can be measured. This can be complicated in reality, especially for tire deflection.

The quadratic performance index is

$$J = \lim_{t\to\infty} E[r_1 y_1^2 + r_2 y_2^2 + r_3 y_3^2], \tag{9}$$

where E denotes the expectation value. It contains the three important performance criteria: Body acceleration y_1, suspension deflection y_2, and tire deflection y_3. While the weight for the body acceleration is fixed at $r_1 = 1$, the weights r_2 and r_3 are varied to influence the optimal tradeoff between ride comfort, suspension travel, and ride safety. The resulting control law is state feedback of the form

$$u^* = -\mathbf{k}^T \mathbf{x}. \tag{10}$$

It is important to notice that in (10) the computed feedback is applied to the *augmented* LBAS model including the filter. The reason for not directly designing the controller for the augmented sixth order system is the structure of the performance index for LQR control, which requires an explicit weight of the control input to be positive definite. The fourth order system fulfills this requirement, since there exists a direct feedthrough from u to y_1. The augmented sixth order system in contrast does not contain such a term. Hence, an explicit weighting of u^* would be necessary to obtain a valid performance index J. However, explicit weighting of the control input would be ineffective because no frequency dependent weight can be introduced in the LQR-controller design framework. But penalizing u^* over the whole frequency range would lead either to inactive controllers for high weights or the effect of the low pass filter would get lost for low weights.

For the determination of the feedback gain $\mathbf{k}^T$ we first rewrite the performance index (9) as

$$\begin{aligned} J &= \lim_{t\to\infty} E\Big[\mathbf{y}^T \underbrace{\operatorname{diag}(1, r_2, r_3)}_{\tilde{\mathbf{R}}} \mathbf{y}\Big] \\ &= \lim_{t\to\infty} E\Big[\mathbf{x}^T \underbrace{\mathbf{C}^T\tilde{\mathbf{R}}\mathbf{C}}_{\mathbf{R_1}} \mathbf{x} + u \underbrace{\mathbf{d}^T\tilde{\mathbf{R}}\mathbf{d}}_{R_2} u + \mathbf{x}^T \underbrace{\mathbf{C}^T\tilde{\mathbf{R}}\mathbf{d}}_{\mathbf{R_3}} u \\ &\quad + u \underbrace{\mathbf{d}^T\tilde{\mathbf{R}}\mathbf{C}}_{\mathbf{R}_3^T} \mathbf{x}\Big]. \end{aligned} \tag{11}$$

With (11) the controller gain vector is derived as

$$\mathbf{k}^T = R_2^{-1}\left(\mathbf{b}^T\mathbf{P} + \mathbf{R}_3^T\right) \tag{12}$$

with $\mathbf{P}$ being the symmetric, positive definite solution of the extended algebraic Riccati equation

$$\mathbf{0} = \mathbf{A}^T\mathbf{P} + \mathbf{P}\mathbf{A} - (\mathbf{P}\mathbf{b} + \mathbf{R}_3) R_2^{-1} (\mathbf{P}\mathbf{b} + \mathbf{R}_3)^T + \mathbf{R}_1 . \tag{13}$$

4. SYSTEM ANALYSIS

The influences of bandwidth and damping on the performance of an LBAS are analyzed in a similar way as presented in Sharp and Hassan (1987). The results are then used in Section 5 to evaluate the potential of LBASs with variable damper using an iterative optimization procedure.

4.1 Normalization

In order to ensure comparability of the systems performance independent of the road excitation, normalized rms values $\tilde{\sigma}$ of the outputs $\mathbf{y}$ are used. Therefore the rms values σ are divided by the square root of the white noise intensity $V_{\dot{x}_g} = 2\pi Av$. For instance the normalized rms value of the body acceleration is

$$\tilde{\sigma}_{y_1} = \frac{\sigma_{y_1}}{\sqrt{2\pi Av}}. \tag{14}$$

4.2 Benchmark systems

Three suspension systems are performance benchmarks for the LBAS with variable damping: The two HBAS designs H and H_1, and a typical passive suspension system P. System H was designed to be optimal in terms of ride comfort, while not exceeding the working space requirements or the tire deflection of P. Design H_1 was synthesized as a minimal body acceleration suspension system adapted to operating conditions characterized by $A = 4.9 \cdot 10^{-6}\,\mathrm{m}$ and $v = 25\,\mathrm{m/s}$. Table 2 summarizes the properties of all benchmark systems.

Table 2. Benchmark systems

Design	ζ_b	$\tilde{\sigma}_{y_1}$	$\tilde{\sigma}_{y_2}$	$\tilde{\sigma}_{y_3}$	r_1	r_2
H	0.30	$26.50\,\mathrm{s}^{-3/2}$	$0.36\,\mathrm{s}^{1/2}$	$0.13\,\mathrm{s}^{1/2}$	1162	53509
H_1	0.30	$11.70\,\mathrm{s}^{-3/2}$	$0.59\,\mathrm{s}^{1/2}$	$0.28\,\mathrm{s}^{1/2}$	96	1531
P	0.30	$31.56\,\mathrm{s}^{-3/2}$	$0.38\,\mathrm{s}^{1/2}$	$0.13\,\mathrm{s}^{1/2}$	–	–
Parameters of all designs according to Table 1						

4.3 Influence of bandwidth

To study the influence of bandwidth the controller weights of design H are applied to the LBAS. Thus, the performance of both systems can be compared. The actuator bandwidth $f_c = \omega_c/2\pi$ is varied from $0.1\,\mathrm{Hz} - 40\,\mathrm{Hz}$ and five different values of body damping ratio ζ_b are assumed.

For the disturbance (8), Figure 3 shows the normalized rms values of all outputs. The graphs start at the values of the associated passive systems and asymptotically reach the performance of the HBAS system H.

Figure 3a) shows remarkably low normalized rms body accelerations obtained with $f_c \approx 3$Hz for lightly damped systems. In terms of suspension deflection (Figure 3b)) this bandwidth shows very good performance especially for systems with low and medium damping. The ride safety performance is shown in Figure 3c). With $f_c \geq 15$ Hz, normalized rms tire deflections can be obtained that nearly achieve the same performance as the HBAS benchmark system H except for very strongly damped suspensions. A cut-off frequency of $f_c \approx 25$ Hz is roughly the limit, where an LBAS almost matches the performance of the HBAS, particularly if the damping is adjustable.

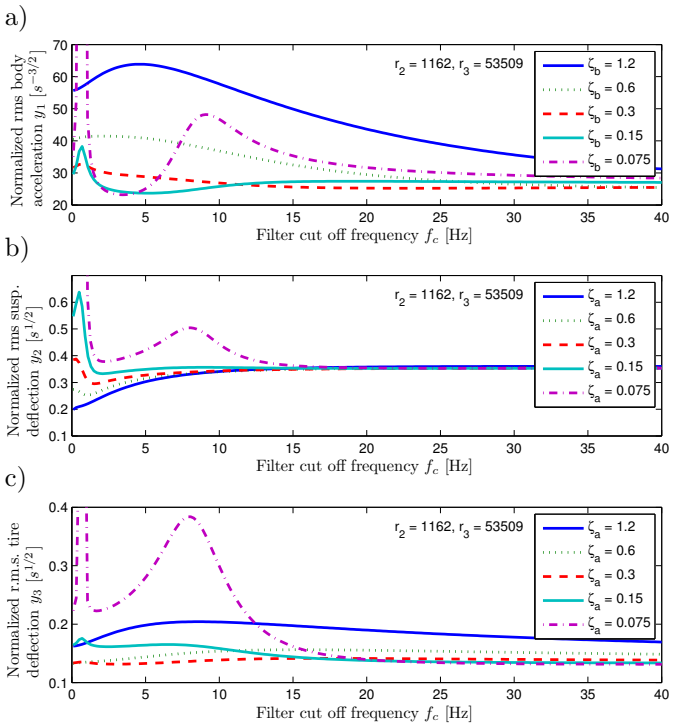

Fig. 3. LBAS performance depending on f_c a) Body acceleration b) Suspension deflection c) Tire deflection

4.4 Influence of damping

The graphs of Figure 3 clearly show, that damping has a wide influence on the performance, especially for low filter cut-off frequencies. Therefore, the right choice of the damping ratio is essential for the design of an LBAS. In many cases adapting the damping ratio has more effect on the outputs than changing the weights of the LQR-control.

This is illustrated in Figure 4 for an LBAS with a filter cut-off frequency of 3 Hz. The two graphs belong to two different sets of weights r_2 and r_3 applied to the bandlimited system. These weights were originally computed for designs H and H_1.

Though the weights differ heavily, the influence on the normalized rms values is only marginal, for a wide range of damping ratios. Only for very low damping ratios, the influence of the controller weights becomes more significant.

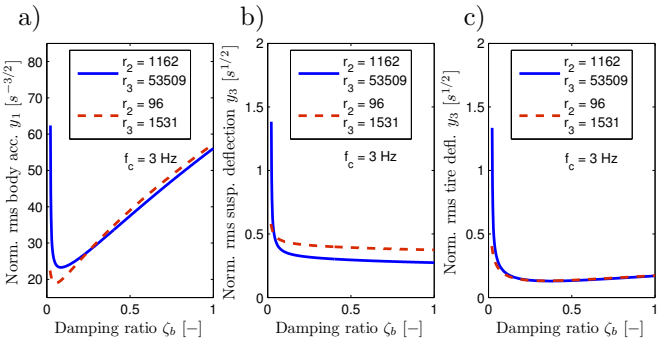

Fig. 4. LBAS performance depending on ζ_b a) Body acceleration b) Suspension deflection c) Tire deflection

5. EVALUATION OF ACHIEVABLE PERFORMANCE

The results of Section 4 are now combined in an iterative optimization of controller weights and damping for specific road conditions in order to point out the potential of LBASs with continuously variable dampers. The adaptation of the damper assists to increase suspension and tire deflection within tolerable bounds for the benefit of lower body acceleration.

5.1 Carpet plots

To find the optimal configuration for each operating condition, carpet plots, originally introduced by Hrovat (1987–1988), together with damping plots like those of Figure 4 are used in an iterative optimization procedure. Carpet plots show the normalized rms body acceleration versus the normalized rms suspension deflection and the tire deflection, respectively. In order to analyze the influence of the weights systematically, one of the two weights, r_2 or r_3, is fixed at a constant value and the other one is varied over a wide range. The resulting weighting net assigns a point in the carpet plot representing a specific suspension performance to a certain pair of weights. Figure 5 shows the carpet plots in their original form, as they are obtained for the HBAS model shown in Figure 2b). The boundary of the weighting nets formed by the curves for $r_2 = 10^{-3}$ and $r_3 = 10^{-2}$ encloses the area of potential suspension performance achievable by varying the controller weights.

Because of the equivalence of LBASs without the low pass filter and HBASs derived in Section 2.2 very similar carpet plots are obtained for LBASs with very high filter cut-off frequencies. For decreasing actuator bandwidths the lower parts of the weighting nets in Figure 5 begin to "fold upwards" and parts of the weighting nets tend to infinity.

These instabilities occur because the control law is applied to the LBAS model including the low pass filter while it was designed for the model without the filter. Figure 6 shows the carpet plots for an LBAS with a filter cut-off frequency of 3 Hz and a body damping ratio of $\zeta_b = 0.30$. As a result of the "folding" the boundary of the area representing the potential suspension performances is now formed by multiple curves, not necessarily being those

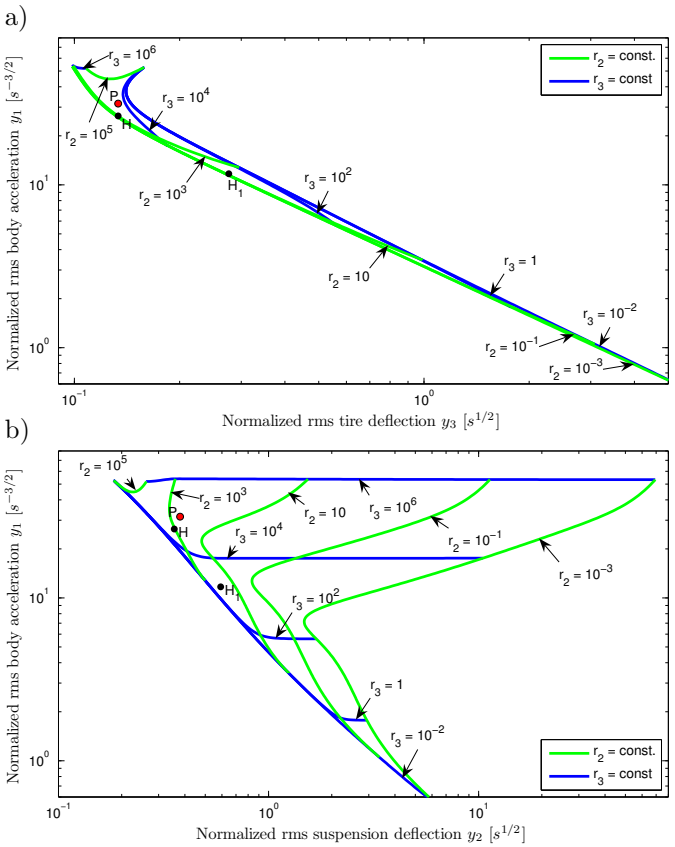

Fig. 5. Carpet Plots for an HBAS.

mapped in the plot. Nevertheless, the maximum area enclosed by all mapped curves remains a good approximation for the achievable performance.

One can use the carpet plots to specify a target performance within the achievable area with respect to one of the constraints, maximum acceptable normalized rms tire deflection or suspension deflection. Then an optimization process can be started, varying r_2 and r_3 until the specified performance is achieved within a predefined tolerance. Since it is only possible to specify a target performance in *one* of the plots it is subsequently necessary to verify that the other constraint is not violated.

5.2 Operating condition dependent constraints

The maximum tolerable values $y_{2,max}$ and $y_{3,max}$ are often transformed into rms constraints by the 3σ-rule

$$\sigma_{y,max} = \frac{y_{max}}{3}. \tag{15}$$

Assuming that y is a normally distributed random variable this assures that y remains within $\pm y_{max}$ for 99.7% of the time, if the rms value $\sigma_{y,max}$ is not exceeded (see e.g. Wirsching et al. (1995)). In order to obtain the *normalized* rms constraints, see Section 4.1.

5.3 Optimization of controller weights and damping

The challenge is to find a setting for damping ratio and controller weights that minimizes the normalized rms body acceleration $\tilde{\sigma}_{y_1}$ without violating $\tilde{\sigma}_{y_2,max}$ and $\tilde{\sigma}_{y_3,max}$. This optimization usually is an iterative procedure, because changing the damping ratio results in modified carpet plots and changing the controller weights results in

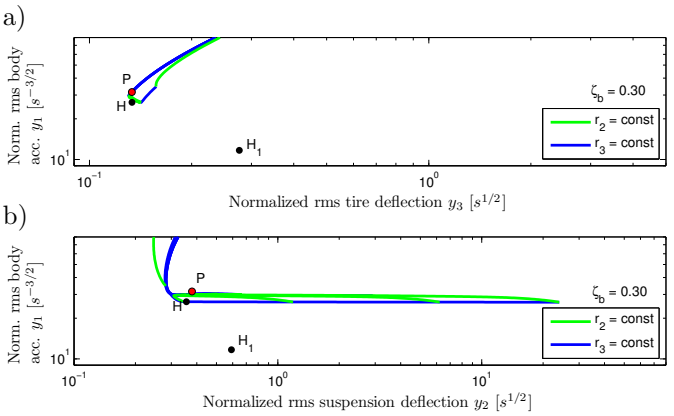

Fig. 6. Carpet Plots for an LBAS ($f_c = 3\,\mathrm{Hz}$, $\zeta_b = 0.30$)

new damping plots. Thus, the damping and the controller weights are alternately optimized until no further enhancement can be obtained. This approach ensures performance improvement in each iteration step and is illustrated by an example.

A vehicle with parameters as in Table 1 is equipped with an LBAS ($f_c = 3\,\mathrm{Hz}$) and a variable damper. The vehicle speed is $v = 25\,\mathrm{m/s}$ and the road roughness coefficient equals $A = 4.9 \cdot 10^{-6}\,\mathrm{m}$. The maximum acceptable suspension travel is $y_{2,max} = \pm 0.08\,\mathrm{m}$ and the tire deflection is limited to $y_{3,max} = \pm 0.023\,\mathrm{m}$ to ensure safety. Using the 3σ-rule (15) and (14), these constraints are normalized to $\tilde{\sigma}_{y_2,max} = 0.961\,\mathrm{s}^{1/2}$ and $\tilde{\sigma}_{y_3,max} = 0.276\,\mathrm{s}^{1/2}$.

The iterative optimization of controller weights and damping ratio for this driving condition is shown in Table 3. As an initial setting, denoted by I, the controller weights of benchmark system H and a damping ratio of $\zeta_b = 0.30$ are chosen. This design represents an "allround" setting, typical for an LBAS with fixed damping, since it offers lower body acceleration than the passive system P at comparable levels of suspension and tire deflection. With variable damping better adaptation to the driving conditions mentioned is possible. Thus, in the first iteration step the damping ratio can be lowered to the acceleration minimum ($\zeta_b = 0.085$) according to Figure 4. Without violating the constraints this results in design $L_{1,a}$.

The carpet plots for this setup (see Figure 7) clearly show that it is possible to further improve ride comfort by adapting the controller weights. Since all acceleration optimal controller weights result in the same tire deflection (see Figure 7a)), the target performance for iteration

Table 3. Optimization example

		I	$\xrightarrow{\text{DA1}} L_{1,a}$	$\xrightarrow{\text{CA1}} L_{1,b}$	$\xrightarrow{\text{DA2}} L_1$	
LQR-weights	r_2	1162	1162	0.0016	0.0016	
	r_3	53509	53509	241	241	
Damping ratio	ζ_b	0.15	0.085	0.085	0.048	
Performance objectives	$\tilde{\sigma}_{y_1}$	29.62	23.29	19.09	18.04	$[\mathrm{s}^{-3/2}]$
	$\tilde{\sigma}_{y_2}$	0.31	0.37	0.44	0.48	$[\mathrm{s}^{1/2}]$
	$\tilde{\sigma}_{y_3}$	0.13	0.22	0.19	0.25	$[\mathrm{s}^{1/2}]$
Comfort gain vs. initial (I)		0%	21.37%	35.55%	39.10%	
Comfort gain vs. passive (P)		6.15%	26.21%	39.51%	42.85%	

step CA1 is specified in Figure 7b) to assure that the constraint for the suspension deflection is not violated. The target performance is set to $\tilde{\sigma}^*_{y_1} = 19.09\,\mathrm{s}^{-3/2}$ and $\tilde{\sigma}^*_{y_2} = 0.444\,\mathrm{s}^{1/2}$. To reach this performance within a tolerance radius of $\epsilon = 2 \cdot 10^{-4}$ in the logarithmical plot the weights are calculated as shown in Table 3. The new intermediate design is denoted by $L_{1,b}$. In order to further improve performance by adapting the damping in the next iteration step (DA2) the damping plots in Figure 8 are used. The acceleration optimal damping ratio, being $\zeta_b = 0.048$, can be chosen and the new design denoted by L_1 results. As the new modified carpet plots in Figure 9 show, no further improvement is possible and hence L_1 is the final design. This iterative adaptation leads to a reduction of normalized rms body acceleration of more than 39% compared to the "allround" LBAS I and more than 42% with respect to the passive suspension P.

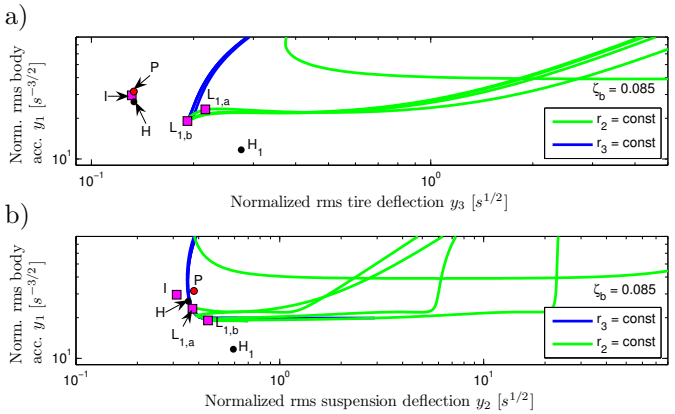

Fig. 7. Carpet Plots for an LBAS ($f_c = 3\,\mathrm{Hz}$, $\zeta_b = 0.085$)

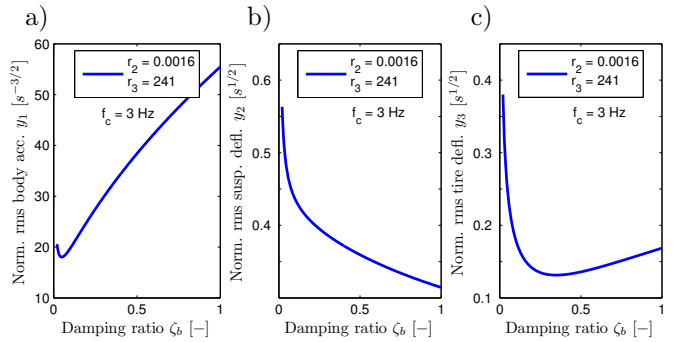

Fig. 8. Damping plot for an LBAS ($f_c = 3\,\mathrm{Hz}$)

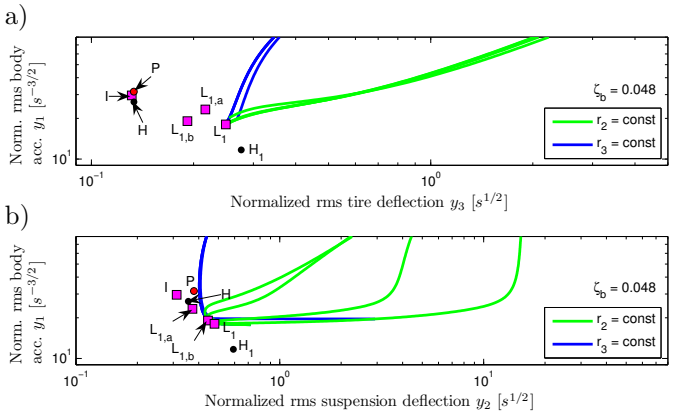

Fig. 9. Carpet Plots for an LBAS ($f_c = 3\,\mathrm{Hz}$, $\zeta_b = 0.048$)

For comparison the performance of all benchmark systems is also marked in the carpet plots. One can see that the HBAS H_1 can fully exploit one of the normalized rms constraints for the benefit of lower body accelerations. In contrast, a limit exists for the LBAS where increasing the suspension or tire deflection does no longer imply lower body accelerations (see Figure 9). To achieve similar performance as H_1 with an LBAS including a continuously variable damper a bandwidth of at least 25 Hz is required. Considering the lower hardware complexity, costs and energy demands of an LBAS with a variable damper, the achievable performance in ride comfort is significant.

6. CONCLUSION

It has been shown that the performance of low bandwidth active suspension systems with variable damper can be optimized by adapting the controller tuning and the damping ratio to the current road excitation. Thereby, safety emphasizing settings improving the performance of passive systems as well as comfort oriented settings, located in performance regions otherwise only accessible to high bandwidth active suspensions, can be offered. First, the influence of actuator bandwidth and damping ratio on the conflicting objectives ride comfort, safety, and suspension travel was analyzed utilizing an LQR-controller for the actuator. Using this results, an iterative optimization procedure for controller weights and damping coefficient has been performed to minimize the normalized rms-value of vertical chassis acceleration while satisfying given constraints on suspension travel and tire deflections.

In an example, a comfort gain of approx. 42% compared to the passive suspension is reached. The availability of the hardware already provides feasibility of the concept. The synthesis of an adaptive suspension controller is current work of the authors. Further performance improvements will be achieved by considering the bandwidth limitations of the LBAS and the frequency dependent human sensitivity to vibrations in the controller design. The simulations will be verified using a quarter-vehicle test rig.

REFERENCES

M. Canale et al. Semi-active suspension control using "fast" model-predictive techniques. *IEEE Trans. Contr. Syst. Technol.*, 14(6):1034–1046, 2006.

D. Hrovat. Influence of unsprung weight on vehicle ride quality. *J. Sound Vibration*, 145(1):497–516, 1987–1988.

D. Hrovat. Survey of advanced suspension developments and related optimal control aplications. *Automatica*, 33 (10):1781–1817, 1997.

H. Kwakernaak and R. Sivan. *Linear Optimal Control Systems*. John Wiley and Sons, Inc., New York, 1972.

M. Mitschke and H. Wallentowitz. *Dynamik der Kraftfahrzeuge*. Springer, Berlin, fourth edition, 2004.

M. Pyper et al. *ABC - Active Body Control*. Verlag Moderne Industrie, Augsburg, 2003.

R. S. Sharp and S. A. Hassan. On the performance of active automobile suspension systems of limited bandwidth. *Vehicle Syst. Dyn.*, 16:213–225, 1987.

P. H. Wirsching et al. *Random Vibrations – Theory and Practice*. John Wiley and Sons, Inc., New York, 1995.

J. Y. Wong. *Theory of Ground Vehicles*. John Wiley & Sons, New York, 2001.